JOURNAL OF CATALYSIS 157, 209–221 (1995)

The Effects of EFAl Extraction on 2-Methylpentane Cracking over Steamed HY

G. R. Bamwenda, Y. X. Zhao, W. A. Groten, and B. W. Wojciechowski[1]

Department of Chemical Engineering, Queen's University, Kingston, Ontario, Canada K7L 3N6

Received January 30, 1995; revised July 1, 1995; accepted July 24, 1995

We have examined the cracking of 2-methylpentane at 400°C on a steamed HY catalyst and on the same catalyst after extraction of its extra-framework aluminum (EFAl) using ammonium hexafluorosilicate. MAS-NMR data show that our procedure removes the EFAl, leaving the framework aluminum (FAl) intact. Kinetic runs on the various catalysts produced by steaming alone and by steaming followed by EFAl extraction have yielded quantitative reaction parameters, which we obtain by fitting the observed conversion and selectivity data with well-defined theoretical equations. The parameters thus obtained show that monomolecular and bimolecular reactions are equally active on both the extracted and unextracted catalysts; the feed is converted by monomolecular and bimolecular reactions in a ratio of ~1 : 2.3 on both catalysts. Closer examination of the kinetic parameters shows that the extraction of EFAl results in an ~30% increase in the total rate of first-order initiation and a much smaller increase in the second-order rate constant for decay, indicating that swaths of sites rather than isolated sites have been activated, or made accessible, by the removal of the EFAl. At the same time, initial product selectivities show that there is no significant change in the nature of the FAl sites after EFAl is removed. None of the individual elementary reactions of the cracking mechanism is affected by the removal of the EFAl. There is therefore no evidence that EFAl participates in a selective way in the cracking of 2-methylpentane under our experimental conditions. We conclude that the role of the EFAl in the cracking of 2-methylpentane is small, involving purely mechanical blocking of a random selection of the active sites, leaving the catalytically active centres at the FAl in an unchanged condition. There is little evidence in our data of any catalytically significant chemical interaction between the Brønsted acid sites residing on the crystal lattice framework and the EFAl. Such evidence as there is comes from the slight increase in the rate of catalyst decay and is discussed in detail.

INTRODUCTION

Zeolites play an important role in oil refining (1); in particular, zeolite Y is a common ingredient in commercial cracking catalysts. Most commercial cracking catalysts contain acid Y zeolite (HY) which has been subjected to framework dealumination by means of a hydrothermal treatment called "steaming" (2, 3) or by using the fluorosilicate technique (4). Owing to a strong industrial interest in various catalyst pretreatment procedures, a number of studies (5–11) have been devoted to the characterization of the physical, chemical, and catalytic properties of dealuminated HY zeolites. However, little is known about the performance of HY which has been dealuminated by steaming, followed by leaching, to obtain an HY containing reduced amounts of extra-framework aluminum (EFAl) (12–15). Such studies are of special interest, because the role of EFAl in the cracking of hydrocarbons is not clear and may be significant.

Here we report the performance of a steam-dealuminated HY, and the same HY after EFAl extraction by ammonium hexafluorosilicate, using the well-studied test reaction of 2-methylpentane cracking (16, 17).

EXPERIMENTAL

The 2-methylpentane (99.0%) was obtained from Aldrich and used without further purification. The only impurity observed was 3-methylpentane (~0.55%). Ultrastable HY (USHY) was prepared from NaY, obtained from BDH Chemicals, by repeated exchange with 0.5 *M* NH_4NO_3 solution at ~20°C for 24 h. Between exchanges, the catalyst was dried at 110°C for 24 h and then calcined in air at 500°C for 2 h. After this procedure was repeated 10 times, samples with a 99+% of the Na^+ exchanged were steamed at various temperatures between 200 and 500°C for periods ranging from 16 to 98 h. The steamed samples were then pelletized, crushed, and sieved to obtain the 60–80 mesh material used as catalyst in our runs.

Ultrastable HY, free of EFAl, was prepared by extracting EFAl using $(NH_4)_2SiF_6$ (AHF). Six grams of USHY was placed in a flask containing 0.45 cm^3 of 0.8 *M* ammonium acetate; 16 cm^3 of 0.5 *M* AHF was added slowly with stirring, giving a final pH of 6.5. The mixture was stirred for 3 h at ~80°C. The catalyst was then filtered and

---

[1] To whom correspondence should be addressed.

0021-9517/95 $12.00

washed thoroughly (15 washes, with the final one lasting 13 h) at 40°C with distilled water. Next, the catalyst was dried overnight in an oven at 110°C. After this treatment, the catalyst was pelletized, crushed, and sized to 60–80 mesh. The catalyst samples were kept in a desiccator over water, i.e., in a water-saturated atmosphere, for 6 h at room temperature before the NMR experiments.

^{27}Al NMR was used to monitor the framework and extra-framework components of the catalysts. ^{27}Al MAS-NMR spectroscopy was done on a Brucker AM-400 spectrometer with Doty solid state accessories at 104.26 MHz. Experimental conditions were PW = 1.2 μs ($2\pi/6$ pulse); RD = 0.5 s; SW = 50 kHz; SI = 4 k data points. A total of 5000 scans were collected for each spectrum at a spinning rate of 10 kHz. ^{29}Si MAS-NMR measurements were carried out on a Brucker CXP200 spectrometer at 39.7 MHz. A pulse of 3 μs and a recycling time of 10 s were applied. The spinning rate was 3 kHz.

The bulk Si/Al ratio of the catalysts was determined by elemental analysis, and the framework of Si/Al ratio was determined by X-ray diffraction. X-ray diffraction measurements were performed on a STOE STADI Z/PL instrument using Cu$K\alpha$ monochromatic radiation ($\lambda(K\alpha_1 = 1.54056)$). As_4O_6 was used as an internal standard.

The 2-methylpentane cracking experiments were carried out in an isothermal plug-flow glass reactor (60 × 2 cm i.d.). Time on stream was varied between 1.5 and 15 min by changing the feed rate of the reactant, but keeping the weight of total feed delivered constant in various runs. Various catalyst-to-reactant ratios were obtained by changing the amount of catalyst in the reactor, the weight of the feed being kept constant. Detailed experimental procedures and analytical techniques have been outlined elsewhere (18).

RESULTS AND DISCUSSION

Effect of Steam Dealumination on the Properties of HY

A number of dealuminated HY samples were obtained by varying the steaming time between 16 and 98 h and the temperature between 200 and 500°C. All samples, except those steamed at temperatures >400°C, showed good crystallinity, as confirmed by X-ray analysis. Unit cell parameters for HY samples steamed in the temperature range 400–500°C were not determined because of the poor quality of the powder patterns, due to structural disorder at the unit cell level.

Chemical Composition and Structure of the Catalyst

The chemical composition and structural parameters of our catalyst are reported in Table 1. As seen in Table 1, the framework Si/Al ratio, estimated from the unit cell parameter by using the equation proposed by Higgins *et al.* (19), increases with steaming time and temperature.

Figures 1a, 1b, and 1d present the ^{27}Al MAS-NMR spectra of HY samples steamed at 200, 300, and 500°C, respectively. The peaks around 44.3, 14.3, and −13.6 ppm correspond to tetrahedral framework alumina, penta- and octahedral-coordinated extra-framework aluminum. As seen in Fig. 1, higher steaming temperatures led to an increase in the intensity for penta- and octahedral-coordinated ETAl groupings.

Figure 2a, 2b, and 2d present ^{29}Si MAS-NMR spectra of the steamed HY samples. Peaks at about −102 and −107 ppm correspond to Si (1Al) and Si (4Al) groupings. A substantial decrease in intensity of the Si (1Al) peak relative to Si (4Al) and a slight shift of the Si (4Al) peak to higher fields was observed with increasing steaming temperature, indicating a gradual removal of framework aluminum with increasing steaming temperature, as shown in Table 1.

Catalytic Activity

A preliminary investigation was carried out in order to gage the cracking activity of each of the samples under the following operating conditions: feed, 2-methylpentane; time on stream, 7.5 min; cat./oil, 0.005 wt/wt; temperature, 400°C.

As shown in Table 1, starting with unsteamed HY, conversion increased to a maximum at sample USHY200-26 (steamed for 26 h at 200°C) and then decreased with increasing duration and temperature of steaming until it reached zero for sample USHY450-98 (steamed for 98 h at 450°C). This type of behavior is strictly in keeping with results published elsewhere (e.g., (20)).

It is well known that cracking on HY is a function of catalyst acidity and site density. The potential number of acid sites is thought to be equal to that of framework Al atoms, but the real number of acid sites depends on the degree of dehydroxylation, on the accessibility of sites, and on sample crystallinity. The dealumination caused by steaming results in an increase of the framework Si/Al ratio, which suggests a decrease in the number of active sites and, since isolated aluminums are expected to be more acidic, a shift in the acid strength of the average remaining active site toward stronger values (21). It will also produce Al-containing debris, which may interact with the active sites on the framework.

On the basis of the above understanding, we can interpret the changes of activity on our HY catalysts as follows:

—In sample USHY200-26, the increase in acid site strength, over that of the acid sites on unsteamed HY, dominates the loss of available sites in its effect on the overall activity, with the result that the overall activity is higher.

—For samples USHY300-24 and USHY300-43, the decrease in site numbers dominates the effect of any further

TABLE 1

Chemical Composition and 2-Methylpentane Cracking Activity of Various HY Zeolite Catalysts

Catalyst[a]	Unit cell[b] parameter (Å)	$(Si/Al)_F$[c]	Aluminum atoms/U.C.[c] (framework)	Conversion[d] (wt%)
HY	24.584	3.73	41	6.90
USHY200-26	24.536	4.49	35	7.21
USHY300-24	24.462	6.13	27	6.69
USHY300-43	24.455	6.35	26	4.77
USHY400-24	—[e]	—	—	1.41
USHY500-24	—[e]	—	—	0.91
USHY450-98	—[f]	—	—	0

[a] The code is USHY (steaming temperature) − (steaming duration). The concentration of Na^+ in all samples was below 240 ppm.

[b] Determined by X-ray diffraction.

[c] Determined according to Kerr and Dempsey's equation in Higgins *et al.* (19).

[d] Time on stream: 7.5 min; c/o: 0.005; temperature: 400°C.

[e] Not determined because of the poor quality of X-ray patterns. The bulk Si/Al ratio for the samples was 2.5 as determined by elemental analysis.

[f] This sample was amorphous.

increase in site strength, with the result that the overall activity is lower.

—For samples USHY400-24, USHY500-24, and USHY450-98 framework collapse causes a sharp decline in activity due to the loss of lattice-resident sites.

The above explanation describes the probable effects of dealumination by steaming on the activity of the framework sites but does not address the effect of the extra-framework aluminum, an oxide which forms from the extracted aluminum ions and remains in the catalyst pores. This debris contains a variety of oxides of aluminum, clearly takes up space in the pores of the crystallites, and may interact with the acidic centres on the partly dealuminated zeolite framework.

Effect of EFAl Extraction on 2-Methylpentane Cracking

The role of EFAl in cracking reactions can be observed by comparing the kinetic properties of steamed catalyst with those of the same catalyst after EFAl extraction. Because of its high activity for 2-methylpentane cracking, as demonstrated by the preliminary runs, sample USHY200-26 was chosen for the kinetic experiments involving the effects of the extraction of EFAl by AHF. A detailed investigation of the kinetics and mechanism of 2-methylpentane cracking over catalysts USHY200-26 and USHY200-26-AHF was therefore carried out. This study was designed to add to our database on the effects of EFAl extraction, a topic which we had previously examined in the cracking of 2,3-dimethylbutane(6) on the same catalysts.

Verification of EFAl Extraction

After EFAl extraction, the ^{27}Al MAS-NMR spectrum of USHY200-26-AHF (Fig. 1c) shows the complete disappearance of the signals due to EFAl, indicating that the sample is free of EFAl. On the other hand, the ^{29}Si MAS-NMR spectrum of the same sample (Fig. 2c) is very similar to that of its parent sample, USHY200-26, confirming that treatment of USHY200-26 with AHF resulted in no significant change of the framework structure, except for a slight decrease in the signal due to Si(1Al).

Selectivity

Experimental product distribution. The products obtained during the cracking of 2-methylpentane on USHY200-26 and on USHY200-26-AHF include H_2, C_1–C_7 paraffins, C_2–C_8 olefins, C_7–C_{12} aromatics, and coke. Of these only H_2, the C_1–C_6 fractions, and coke were found to be primary products. Initial weight selectivities for all products were obtained by drawing optimum performance envelopes (OPEs) for the products and determining selectivity behavior at zero conversion (22). Figures 3 and 4 show some examples of the OPE plots which are observed in 2-methylpentane cracking over USHY200-26 and USHY200-26-AHF, respectively. The measured initial weight selectivities and, derived from these, the calculated molar selectivities for all primary products, for both catalysts, are shown in Table 2.

No significant difference was observed between the experimental selectivities of the two catalysts. On both

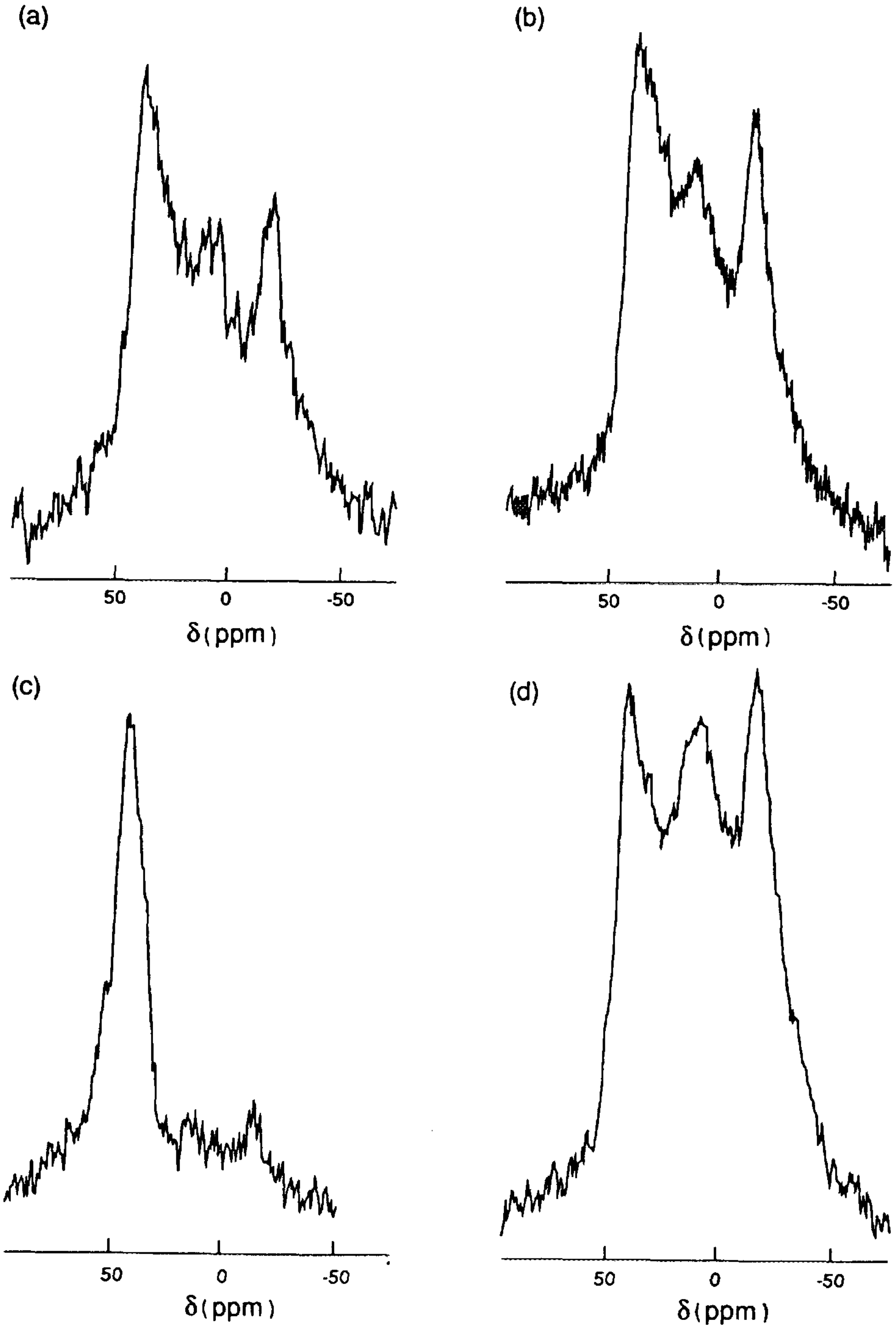

FIG. 1. ^{27}Al MAS-NMR spectra of: (a) USHY200-26; (b) USHY300-24; (c) USHY200-26-AHF; (d) USHY500-24.

catalysts the primary products consist mostly of skeletal isomers of the feed, i.e., 3-methylpentane, 2,3-dimethylbutane, and *n*-hexane, all of which contribute a total of about 60% of the initial products. Other significant primary products consist of C_3–C_5 paraffins and C_6-olefins. However, since each of the products can arise from more than one elementary reaction, in order to understand the effect of the EFAl we must examine the mechanism responsible for the overall process.

Overall reaction mechanism. As has been shown elsewhere (16), 2-methylpentane cracking on USHY follows a chain mechanism involving both monomolecular and bi-

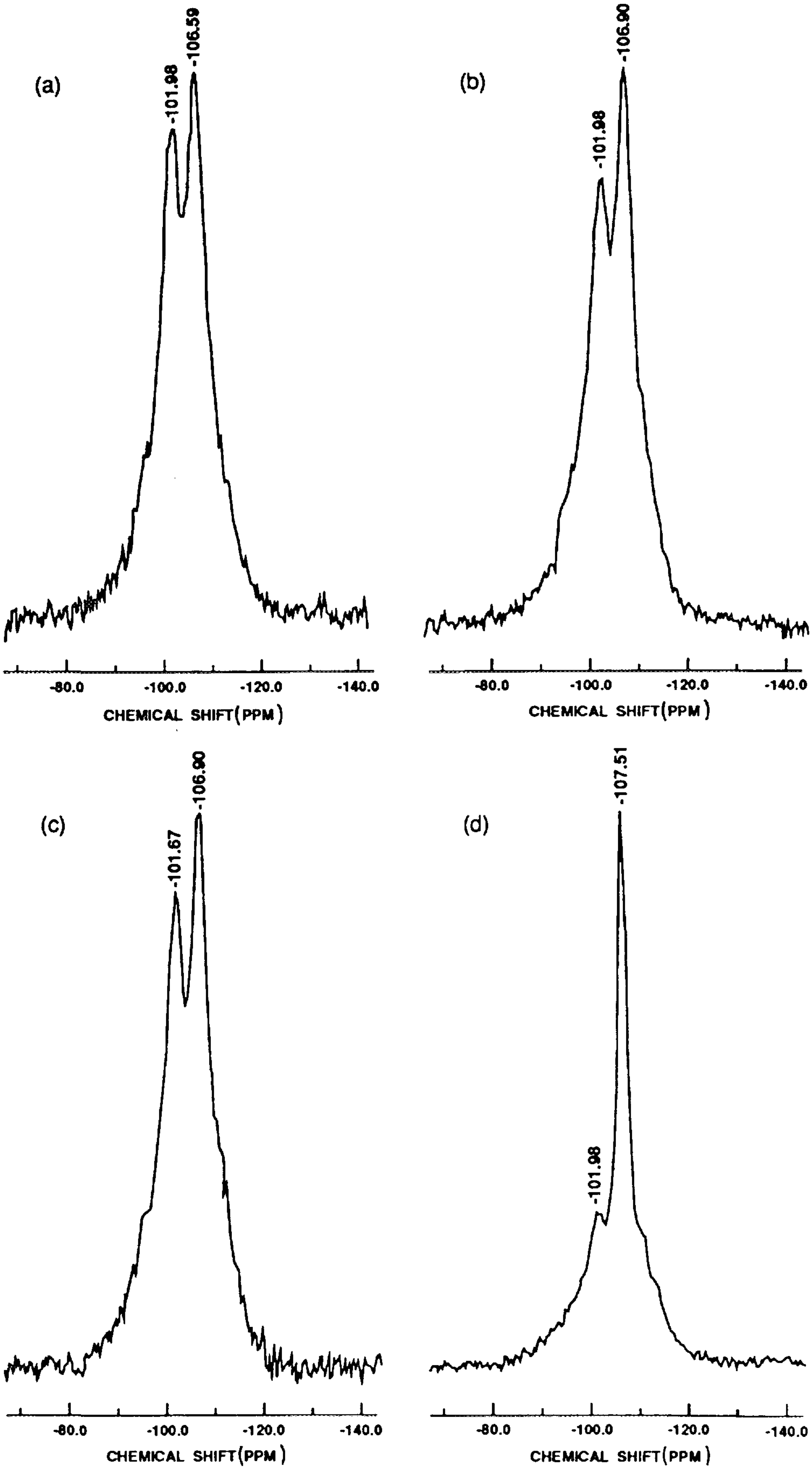

FIG. 2. ^{29}Si MAS-NMR spectra of various zeolites: (a) USHY200-26; (b) USHY300-24; (c) USHY200-26-AHF; (d) USHY500-24.

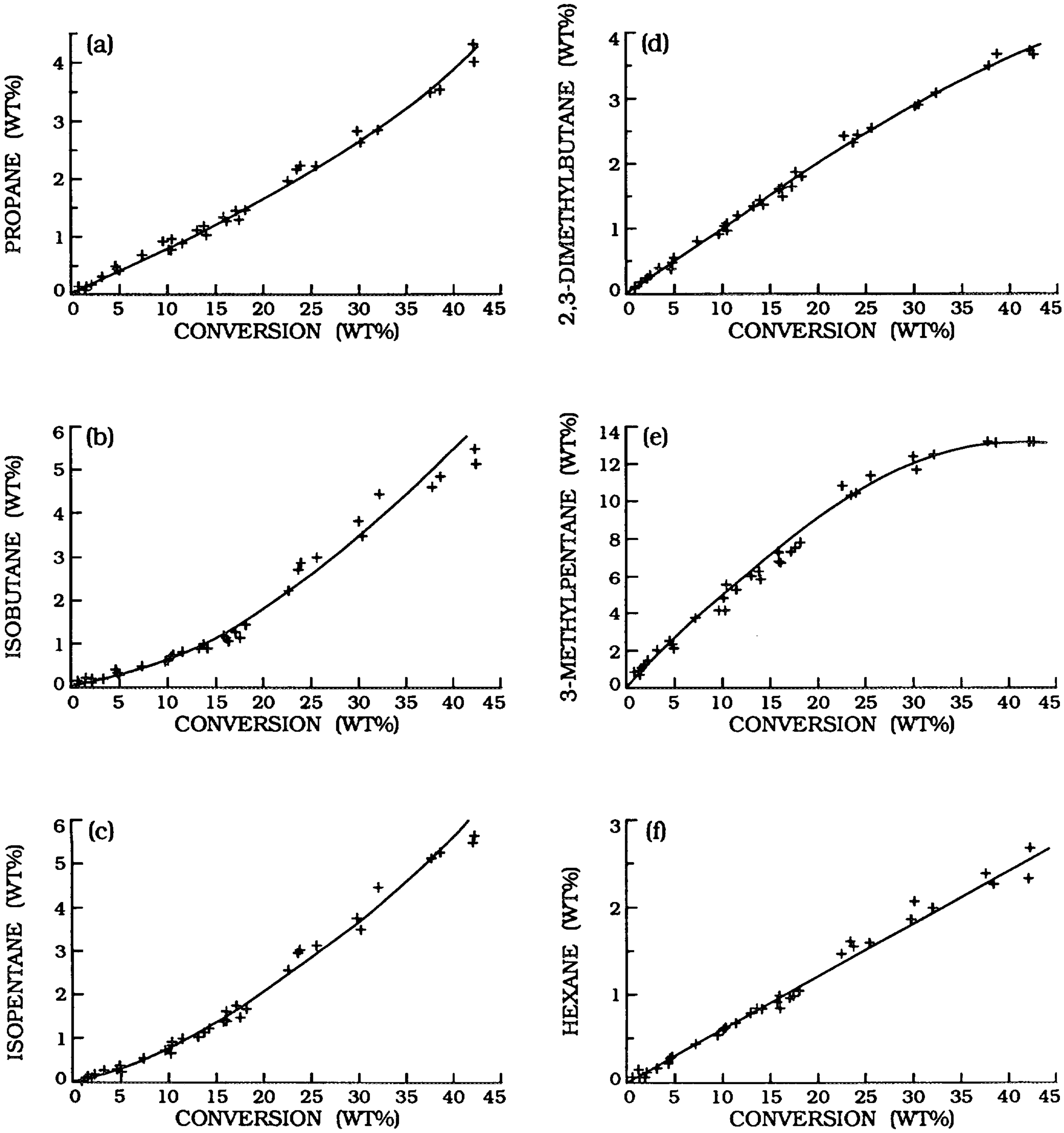

FIG. 3. Optimum performance envelopes for products of reaction of 2-methylpentane on USHY200-26 at 400°C. Catalyst-to-reactant ratio 0.002–0.104.

molecular modes of reaction. The reaction sequence is initiated by the protonation of 2-methylpentane at a Brønsted acid site, forming a carbonium ion. Hydrogen or a small paraffin is then cracked out of the molecule by the protolytic cleavage of a C—H or a C—C bond, leaving a carbenium ion on the Brønsted site, as per the general equation

$$C_6H_{14} + H^+B^- \rightleftarrows C_6H_{15}^+B^- \rightarrow C_iH_{2i+2} + C_{6-i}H_{13-2i}^+B^-, \qquad [1]$$

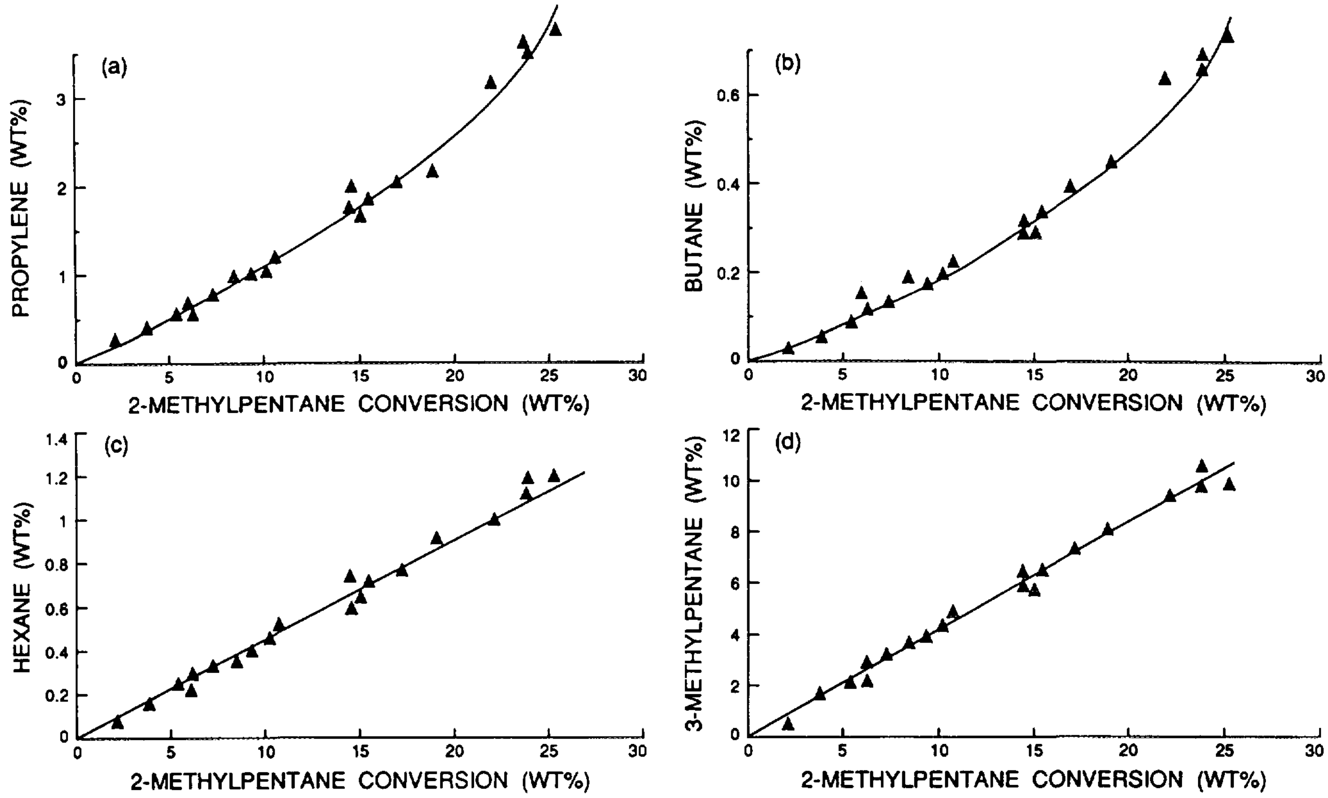

FIG. 4. Optimum performance envelopes for products of reaction of 2-methylpentane on USHY200-26-AHF at 400°C. Catalyst-to-reactant ratio 0.0046–0.0445.

where $i = 0, 1, 2, 3, 4$; $C_6H_{15}^+B^-$ and $C_{6-i}H_{13-2i}^+B^-$ denote carbonium and carbenium ions, respectively.

The larger of the set of possible carbenium ions formed by reaction [*1*] can undergo skeletal rearrangement: i.e., methyl and hydride shifts

$$C_jH_{2j+1}^+B^- \rightleftarrows \text{iso-}C_jH_{2j+1}^+B^-, \qquad [2]$$

where iso-$C_jH_{2j+1}^+B^-$ is the isomerized carbenium ion.

Any such carbenium ion can participate in a chain of reactions propagated by the abstraction of a hydride ion from a feed molecule. This process leads to the formation of a product paraffin and a new *parent* carbenium ion, which can in turn continue to propagate the chain of disproportionation reactions. In general,

$$C_jH_{2j+1}^+B^- + C_6H_{14} \rightarrow C_jH_{2j+2} + C_6H_{13}^+B^-. \qquad [3]$$

For example, hydride abstraction by iso-$C_6H_{13}^+B^-$ species, parent carbenium ions which have undergone a methyl and hydride shift while adsorbed on the active sites, is responsible for the isomeric C_6 paraffins found in the products:

$$\text{iso-}C_6H_{13}^+B^- + C_6H_{14} \rightarrow \text{iso-}C_6H_{14} + C_6H_{13}^+B^-. \qquad [4]$$

Moreover, any carbenium ion formed by reaction [*1*] can also react with a feed molecule by a disproportionation, i.e., by abstracting a carbon-containing moiety from a feed molecule, to produce an alkane and a new carbenium ion;

$$C_jH_{2j+1}^+B^- + C_6H_{14} \rightarrow C_mH_{2m+2} + C_{j+6-m}H_{2j+13-2m}^+B^-, \qquad [5]$$

where $m < 7$, since C_7–C_{11} products were not observed among the primary products of 2-methylpentane cracking on either USHY200-26 or USHY200-26-AFH at 400°C. Finally, the carbenium ion can desorb as an olefin:

$$C_jH_{2j+1}^+B^- \rightleftarrows C_jH_{2j} + H^+B^-. \qquad [6]$$

This process terminates the reaction chain on that site and donates a proton back to the catalyst to reconstitute a Brønsted site.

The lifetime of an individual carbenium ion on the surface depends on the strength of the conjugate base of the acid site on the catalyst lattice, on the reaction temperature,

TABLE 2

Initial Weight and Molar Selectivities for 2-Methylpentane Cracking over USHY200-26 and USHY200-26-AHF at 400°C

	Initial weight selectivity		Initial molar selectivity	
Product	USHY200-26	USHY200-26-AHF	USHY200-26	USHY200-26-AHF
H_2	0.0003	0.0004	0.0129	0.0172
Methane	0.0027	0.0025	0.0145	0.0134
Ethane	0.0017	0.0020	0.0049	0.0057
Ethene	0.0059	0.0054	0.0181	0.0166
Propane	0.0920	0.0956	0.1801	0.1869
Propene	0.0972	0.1020	0.1990	0.2089
C_4-paraffins	0.0758	0.0807	0.1124	0.1197
C_4-olefins	0.0098	0.0100	0.0150	0.0154
C_5-paraffins	0.0861	0.0862	0.1028	0.1030
C_5-olefins	0.0065	0.0067	0.0080	0.0082
C_6-paraffins	0.5712	0.5574	0.5712	0.5574
C_6-olefins	0.0400	0.0410	0.0410	0.0420
Coke	0.0080	0.0087	0.0080	0.0087
Total	0.9972	0.9986	1.2879	1.3031

on the nature of the ion, and on the presence of materials which may encourage desorption. One can expect therefore that the residence time of a carbenium ion is larger on catalyst surfaces with weak conjugate bases (i.e., strong Brønsted acid sites) and at low reaction temperatures (10, 16).

At high reaction temperatures, a large carbenium ion may also undergo β-cracking, to form an olefin and a smaller carbenium ion (16),

$$C_6H_{13}^+B^- \rightarrow C_nH_{2n} + C_{6-n}H_{13-2n}^+B^-, \qquad [7]$$

where $n = 2, 3, 4$. In 2-methylpentane cracking on both USHY200-26 and USHY200-26-AHF at 400°C this reaction does not occur, as we will see.

One more reaction that must be taken into account is the formation of coke, which can be written as the overall process

$$C_jH_{2j+1}^+B^- + C_mH_{2m+1}^+B^- \rightarrow C_jH_{2j-1}^+B^- + C_mH_{2m+2} + H^+B^-. \qquad [8]$$

Since coke is a minor primary product in this reaction, we will use a simplified reaction for the interpretation of experimental selectivity data:

$$C_6H_{14} \rightarrow \text{coke}. \qquad [9]$$

Reaction path probabilities (*RPP*). The chain mechanism described in the preceding section consists of three major parts, i.e., initiation (reaction [*1*], propagation (reactions [*3*], [*4*], [*5*], and termination (reaction [*6*]). A full set of the pertinent elementary reactions for 2-methylpentane cracking on both USHY200-26 and USHY200-26-AHF is presented in Table 3. The RPPs of all individual reaction paths for our system have been calculated using the experimental selectivity data reported in Table 2 and the established methodology (16).

These results are also presented in Table 3. It should be pointed out that in Table 3 some products are seen to be formed by more than one elementary process. In view of this, it is often misleading to comment on the overall mechanism of the reaction on the basis of experimental product selectivities.

Examination of the RPPs presented in Table 3 shows that protolysis on Brønsted acid sites (RPPs X_{00} to X_{04}) accounts for about 30% of the total conversion of feed, while the total of all bimolecular disproportionations accounts for about 70% of the conversion on both USHY200-26 and USHY200-26-AHF. Moreover, there are no significant differences between any of the individual RPP values on the two catalysts. Such differences as are seen in Table 3 are within experimental error. This result leads us to conclude that the two catalysts follow the same mechanism of cracking.

The absence of a significant difference in any individual RPP on the two catalysts indicates that extra-framework aluminum plays no significant role in changing the acid strength distribution of the active sites. We have previously reported that the cracking of 2,3-dimethylbutane on extracted and unextracted catalysts (6) is also unaffected, in agreement with the above observations. The absence of

TABLE 3

Reaction Scheme and Reaction Pathway Probabilities of 2-Methylpentane over USHY200-26 (A) and USHY200-26-AHF (B) at 400°C

Entry No.	Reaction path	RPP values A	RPP values B
1	$C_6H_{14} + H^+B \xrightarrow{X_{00}} H_2 + C_6H_{13}^+B^-$	0.005	0.005
2	$\xrightarrow{X_{01}} CH_4 + C_5H_{11}^+B$	0.014	0.013
3	$\xrightarrow{X_{02}} C_2H_6 + C_4H_9^+B$	0.005	0.006
4	$\xrightarrow{X_{03}} C_3H_8 + C_3H_7^+B^-$	0.148	0.154
5	$\xrightarrow{X_{04}} C_4H_{10} + C_2H_5^+B$	0.109	0.115
	Total monomolecular initiation processes	0.281	0.293
6	$C_6H_{14} + C_2H_5^+B \xrightarrow{X_{20}} C_2H_6 + C_6H_{13}^+B$	0.000	0.000
7	$\xrightarrow{X_{21}} C_3H_8 + C_5H_{11}^+B$	0.000	0.000
8	$\xrightarrow{X_{22}} C_4H_{10} + C_4H_9^+B$	0.003	0.005
9	$\xrightarrow{X_{23}} C_5H_{12} + C_3H_7^+B^-$	0.089	0.093
10	$C_6H_{14} + C_3H_7^+B \xrightarrow{X_{30}} C_3H_8 + C_6H_{13}^+B$	0.031	0.033
11	$\xrightarrow{X_{31}} C_4H_{10} + C_5H_{11}^+B^-$	0.000	0.000
12	$\xrightarrow{X_{32}} C_5H_{12} + C_4H_9^+B$	0.007	0.005
13	$C_6H_{14} + C_4H_9^+B^- \xrightarrow{X_{40}} C_4H_{10} + C_6H_{13}^+B^-$	0.000	0.000
14	$\xrightarrow{X_{41}} C_5H_{12} + C_5H_{11}^+B^-$	0.000	0.000
15	$C_6H_{14} + C_5H_{11}^+B^- \xrightarrow{X_{50}} C_5H_{12} + C_6H_{13}^+B^-$	0.006	0.005
16	$C_6H_{14} + \text{iso-}C_6H_{13}^+B^- \xrightarrow{X_{60}} \text{iso-}C_6H_{14} + C_6H_{13}^+B^-$	0.571	0.557
	Total bimolecular chain processes	0.707	0.698
17	$C_6H_{14} \xrightarrow{X_{kc}} \text{Coke}$	0.012	0.009
18	$C_6H_{13}^+B \xrightarrow{X_{h63}} C_3H_6 + C_3H_7^+B$	0.000	0.000

an effect on selectivity does not preclude the existence of other kinetic effects.

Kinetics

It has been variously reported that the effect of EFAl on catalyst activity is positive (23, 24), negative (11, 25), or dependent on the level of EFAl extraction (13). We will presently see that the EFAl produced by steaming in our samples may block some pores or cover swaths of individual sites but, as we have already seen, it does not affect selectivity.

A kinetic model suitable for this system has been proposed previously (18). The model accounts for monomolecular and bimolecular cracking, both of which are active in 2-methylpentane cracking. It assumes that the same sites catalyze both mechanisms and that a surface reaction is rate-controlling. The model yields the equation

$$\frac{dX}{d\tau} = \frac{[1 + Gt]^{-N}[A_1(1 - X)/(1 + \varepsilon X) + A_2[(1 - X)/(1 + \varepsilon X)]^2}{1 + B(1 - X)/(1 + \varepsilon X)}, \qquad [1]$$

where X is the instantaneous fraction of reactant converted, t is the space time, G is the deactivation rate constant, N is the decay exponent, and ε is the volume expansion coefficient. The constants A_1, A_2, and B are defined by the expressions

$$A_1 = \frac{(\Sigma_i k_{Mi} K_A) + [\Sigma_i(\Sigma_i k_{cj}) K_{Pi} \mathcal{F}_i] C_{A0}}{1 + \Sigma_i K_{Pi} \mathcal{F}_i C_{A0}} [S_0] \qquad [2]$$

$$A_2 = \frac{-[\Sigma_i(\Sigma_i k_{cj}) K_{Pi} \mathcal{F}_i] C_{A0}}{1 + \Sigma_i K_{Pi} \mathcal{F}_i C_{A0}} [S_0] \qquad [3]$$

$$B = \frac{[K_A - (\Sigma_i K_{Pi} \mathcal{F}_i)] C_{A0}}{1 + \Sigma_i K_{Pi} \mathcal{F}_i C_{A0}} [S_0] \qquad [4]$$

where:

k_{Mi} is the rate constant of a feed molecule undergoing the ith mode of monomolecular protolysis;

k_{cj} is the rate constant of a carbenium ion $C_jH_{2j+1}^+$ and a feed molecule; undergoing the jth mode of disproportionation;

K_A is the adsorption constant of a feed molecule;

K_{Pi} is the adsorption constant of the ith product;

C_{A0} is the initial concentration of reactant;

$[S_0]$ is the initial concentration of active sites;

$\mathcal{F}_i$ is the experimental molar selectivity of the ith product.

Experimental conversions for the reaction of 2-methylpentane on USHY200-26 and USHY200-26-AHF at 400°C have been fitted using Eq. [1] and the resultant fit is shown in Figs. 5 and 6. Optimum values of the parameters A_1, A_2, B, and G were determined using the sum of squares of residuals as a criterion of fit and are given in Table 4. The value of the decay exponent N was found to be close to one; its value was therefore fixed at 1.0 for both catalysts (22). The units of catalytic reaction rate parameters are often poorly defined. In order to establish a well-defined set of units, a detailed discussion of the applicable units used to derive parameters from the above rate equation is presented in the Appendix.

In Table 4 it can be seen that the two values of the parameter A_1 are quite similar, indicating that the total activity via monomolecular and bimolecular processes changes only slightly due to the treatment of USHY200-26 with AHF.

Parameter A_2 is necessary in both cases, indicating that the contribution of a chain mechanism is important for both catalysts, as was already evident from the selectivity data discussed above. Although the value of A_2 is a somewhat larger absolute number for USHY200-26 than for USHY200-26-AFH, we do not attach major significance to this in view of the strong correlation between the A_1 and A_2 parameters in the kinetic rate expression. In fact,

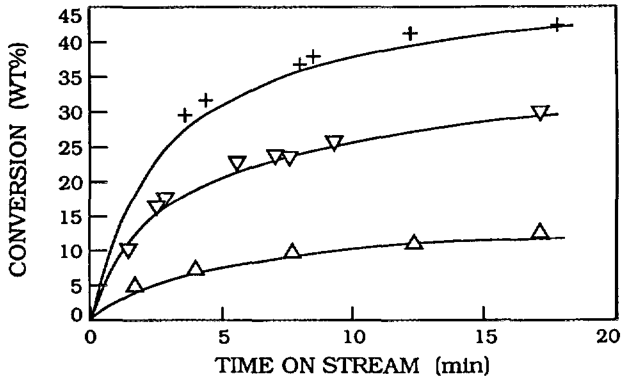

FIG. 5. Theoretical curves and experimental points for the reaction of 2-methylpentane on USHY200-26 at 400°C. Catalyst-to-reactant ratios: △, 0.0077; ▽, 0.043; +, 0.104.

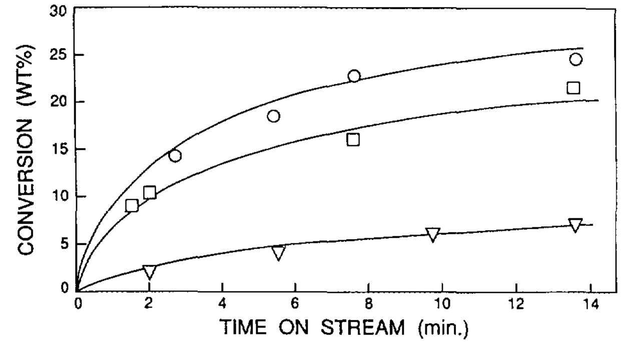

FIG. 6. Theoretical curves and experimental points for the reaction of 2-methylpentane on USHY200-26-AHF at 400°C. Catalyst-to-reactant ratios: ▽, 0.0046; □, 0.0081; ○, 0.0445.

TABLE 4

Optimum Values of Kinetic Parameters in the Cracking of 2-Methylpentane over USHY200-26 and USHY200-26-AHF

Kinetic parameters	USHY200-26	USHY200-26-AHF
$A_1(\mathrm{min}^{-1})^a$	0.355	0.332
$A_2(\mathrm{min}^{-1})^a$	−0.031	−0.027
B	−0.960	−0.972
$G(\mathrm{min}^{-1})^a$	0.251	0.279
N^b	1.0	1.0
$\Sigma \mathcal{F}_i$	1.2879	1.3031
$C_{A0}(\mathrm{mol\ dm}^{-3})$	0.0181	0.0181
$\frac{A_1 + A_2}{1 + B}$ (min^{-1})	8.10	10.89
$\frac{K_A}{K_P}^c$	0.0515	0.0365

[a] See Appendix for explanation of units.
[b] N was fixed at 1.0 for both catalysts.
[c] Determined according to Eq. [15].

these two parameters are always highly correlated in our treatment and are not of much use in establishing the details of the reaction mechanism. Kinetics can only yield information on the total initial rate, relative adsorption strengths of the feed and the average product, and the rate and nature of the decay process. The relative contributions of propagating and initiating reactions should be ascertained from selectivity data.

The parameter B in the model reflects the relative values of adsorption constants of the reactant and products (18). On both catalysts the values of the B parameter are close to -1, indicating that there is strong preferential adsorption of the product species.

Examination of Eq. [4] reveals that the large negative values for B require that both

$$\Sigma K_{\mathrm{P}i} \mathcal{F}_i C_{A0} \gg 1 \qquad [5]$$

and

$$\Sigma K_{\mathrm{P}i} \mathcal{F}_i \gg K_A . \qquad [6]$$

Equation [4] therefore reduces to

$$B = \frac{K_A}{\Sigma K_{\mathrm{P}i} \mathcal{F}_i} - 1 \qquad [7]$$

and

$$B + 1 = \frac{K_A}{\Sigma K_{\mathrm{P}i} \mathcal{F}_i} = \frac{K_a}{K_p \, \Sigma \, \mathcal{F}_i}, \qquad [8]$$

where $p = \Sigma K_{\mathrm{P}i} / \Sigma \, \mathcal{F}_i$ is the weighted average adsorption constant for product species. $\Sigma \, \mathcal{F}_i$ can be calculated from the sum of the molar selectivities of initial products and is given in Table 4. By rearranging Eq. [8] we get

$$\frac{K_A}{K_P} = (B + 1) \, \Sigma \, \mathcal{F}_i . \qquad [9]$$

From Eq. [9], values representative of the ratio of the adsorption constants for feed and the average product have been calculated and are listed in Table 4. It can be seen that the value of K_A/K_P for USHY200-26-AHF is larger than that for USHY200-26, indicating that USHY200-26-AFH may adsorb products more strongly than USHY200-26. Unfortunately, this conclusion is none too firm in this instance since the value of B is close to -1.0 in both cases, making small differences in its fitted value inordinately significant when applied in Eq. [9].

The sum of the rates of all initiating reactions (i.e., all protolysis reactions) can be evaluated with more certainty by using Eq. [1] under the condition of $\tau = 0$ and $X = 0$, i.e.,

$$\left(\frac{dX}{d\tau}\right)_{\tau \to 0} = \frac{A_1 + A_2}{1 + B} . \qquad [10]$$

Despite the strong correlation between A_1 and A_2, this estimate of the rate of initiation is fairly robust. The calculated value of the sum of initiating rates presented in Table 4 shows that USHY200-26-AHF is ~35% more active for 2-methylpentane protolysis than is USHY200-26. In the previous study of 2, 3-dimethylpentane cracking (6) it was found that the extracted catalyst was ~88% more active than the equivalent catalyst containing EFAl. In that case too, there was no significant difference in selectivity between the two catalysts.

The enhancement in activity, as measured by Eq. [10], suggests that the removal of EFAl makes more sites available for protolysis. However, we see that the extracted catalyst does not show increased activity for protolysis alone. From the fact that the selectivity is not altered for any of the products we see that it is the number of *average-strength* sites that is increased and that the increase in the rate of protolysis is accompanied by an equal increase in all other rates of reaction. Otherwise, if the rate of protolysis was enhanced without an equal enhancement in the rate of each of the chain-propagating reactions, we would observe changes in product selectivities.

The much smaller increase in the rate of catalyst decay, as evidenced by the 10% increase in the G parameter of the hyperbolic decay function, suggests that site density is not increased to any great extent by dealumination. The hyperbolic decay function with $N = 1$ indicates that catalyst decay is second order in active site concentration (26–28). If the surface density of active sites were increased by the removal of EFAl, the rate of decay would be expected to increase more rapidly than the rate of cracking, which is first order in site concentration. Rather, it seems, areas of contiguous sites are freed, so that the rate of protolysis, which depends on the number of sites, increases, while catalyst decay, which is more sensitive to site density, increases much less. This suggests to us that the extraction of EFAl simply clears blockades of average assemblies of sites, rather than unblocking individual sites with specific properties. It either unplugs pores, allowing sites trapped behind the blockade to become active, or uncovers patches of sites which had been blanketed by the EFAl debris, or both. A similar result was obtained in the cracking of 2, 3-dimethylbutane where on dealumination the decay constant G increased by 20% while protolysis increased by 88%.

The slight increase, cited above, in the relative size of the equilibrium constant for the adsorption of products agrees with the observed increase in the rate of catalyst decay. Decay in the cracking of 2-methylpentane proceeds by a process which is second order in site concentration, as evidenced by the $N = 1$ value of the decay exponent (16). In such a case any increase in site coverage will result in an increase in the rate of decay. It seems that the increased adsorption of products leads to a higher surface coverage by carbenium ions and hence to an increase in decay, but does not distort the experimental selectivity for the *initial* products; this is measured under conditions where there are no products present. A similar observation was made in the 2,3-dimethylbutane cracking study.

Our results may yet turn out to be specific to the method of dealumination employed. It may turn out that other forms of dealumination produce debris which cover sites in a more selective manner. If that turns out to be the case, it is possible to imagine a catalyst which, on EFAl extraction, will show a greater increase in its decay rate than in its rate of conversion. In that case, extraction would result in a reduction in activity at higher conversion, no effect in a range of conditions where the increase in activity just cancels the increase in decay, or an effect dependent on the level of extraction as the two countervailing effects of extraction come to a trade-off under some "standard" test conditions. Since such varied observations on the effects of extraction have in fact been reported, it may be that small "insignificant" details of the method of dealumination have a major impact on the kind of EFAl produced and its interaction with the sites. This problem merits careful quantitative reconsideration if catalyst modification by EFAl removal is to be useful as a means of catalyst modification.

CONCLUSIONS

An investigation of various steamed HY zeolites in 2-methylpentane cracking at 400°C indicates that higher streaming temperature and longer steaming duration lead to higher framework Si/Al ratios and more EFAl, a fact well documented in the literature (29, 30). Proper streaming increases the observed cracking activity of HY in 2-methylpentane cracking, probably due to an optimum in the adjustment of the opposite effects of site strength and site density. Additional streaming, past the optimum point, decreases the overall cracking activity, probably due to a decrease in the number of sites which is not adequately compensated for by an increase in site strength. Oversteaming decreases cracking activity to zero or very near zero, due to the collapse of the crystallite framework of the zeolite.

A detailed study of the kinetics and selectivity of 2-methylpentane cracking over USHY200-26 and USHY200-26-AFH shows that the extraction of EFAl from the steamed HY results in no significant change of selectivity, but does induce an increase in the total rate of the protolysis reactions in 2-methylpentane cracking. We conclude that we have no evidence of the participation of extra-framework aluminum in altering the suite of cracking reactions of 2-methylpentane on USHY at 400°C. The role of the EFAl is one involving a purely mechanical blocking of pores or of swaths of sites, thereby making more of the average selection of the existing sites unavailable for catalyzing the reaction.

The combination of the increase in the rate of protolysis and the lack of change in selectivity will result in an overall increase in conversion at all levels of conversion under a given set of reaction conditions. This effect is somewhat reduced by a simultaneous increase in the rate of decay. In our catalysts, the increase in the rate of decay is smaller than that in the rate of conversion, but its effects, as usual, are more noticeable at longer times on stream. As a result the benefits of the enhancement in activity are most pronounced at short times on stream. We expect this behavior to be found in all cases of nonselective site blockage.

Steric constraints induced by EFAl may well alter selectivity in reaction systems where shape selectivity of the feed or the size of the transition state in the semiblocked pores turns out to be important. We expect such effects to be more important in the cracking of large molecules, in the formation of complex bimolecular transition states, or in the formation of coke or its precursors.

The extraction of EFAl may also have effects quite different from those reported here if the process of dealumination is different and produces selective site blockage by the EFAl. There is no firm evidence of such a process. Just how such selective EFAl may be intentionally produced is not clear.

APPENDIX

The formal units of the rates of reaction in Table 4 are simply reciprocal time, but in fact they depend on the units used for time-on-stream and on the assumed ratio of feed/catalyst density. This comes about as follows.

We fit our experimental data using Eq. [1]. Thus the rate is in units of

$$\text{mole fraction converted} \times \text{time}^{-1}.$$

Since the mole fraction is dimensionless, the formal units of the rate are simply

$$\text{time}^{-1}.$$

However, this does not tell the whole story. The value of τ is calculated from the cat./oil ratio and the time on stream:

$$\tau = b \times P \times t_f.$$

The time-on-stream is normally recorded in minutes and is responsible for the formal units of the rate. The cat./oil ratio in our work is in units of

weight of catalyst/weight of feed.

Despite the formal cancellation of these units, it must be a weight ratio if one wishes to compare other data to ours. A cat./oil ratio in terms of volume for example will introduce a constant offset from our reported rates. Moreover, b is the ratio of

catalyst density/feed density.

If one wishes to estimate the time that the vaporized feed would spend in the volume occupied by the catalyst one must use feed vapor density here. The absolute value of this number is no particularly meaningful and we have chosen to take

$$b = 1.$$

This assumption is unstated but common in catalytic literature and, if need be, all our rates can be multiplied by a suitable constant value of b to satisfy other assumptions. Many reports in the literature give rates in units of

moles of feed/(gram catalyst × time).

Such units can be retrieved from our data by changing our cat./oil ratio to units of

grams of catalyst/mode of feed.

To do this one would multiply our weight-on-weight cat./oil ratio by the ratio

grams of feed/mole of feed.

This would make the units of contact time

$$\tau = b \times (\text{grams of catalyst/grams of feed}) \times (\text{grams of feed/mole of feed}) \times \text{time};$$

i.e., the units of τ would become

(grams of catalyst/mole of feed) × time.

We see that the numbers in Table 4 would have to be divided by grams of catalyst/mole of feed, that is, by the molecular weight of the feed, in order to arrive at the commonly reported units

moles of feed/(gram catalyst × time).

REFERENCES

1. Wojciechowski, B. W., and Corma, A., "Catalytic Cracking: Catalysts, Chemistry, and Kinetics." Dekker, New York, 1986.
2. Scherzer, J., *in* "Catalytic Material: Relationship between Structure and Reactivity," ACS Symposium Series No. 248, p. 157. Am. Chem. Soc., Washington, DC, 1984.
3. Scherzer, J., *Catal. Rev.-Sci. Eng.* **31**(3), 215 (1989).
4. Skeels, G. W., and Breck, D. W., *in* "Proceedings, 6th International Zeolite Conference, Reno, Nevada," p. 87. Butterworths, London, 1984.
5. Bamwenda, G. R., Groten, W. A., and Wojciechowski, B. W., *Stud. Surf. Sci. Catal.* **68**, 753 (1991).
6. Bamwenda, G. R., Zhao, Y. X., and Wojciechowski, B. W., *J. Catal.* **150**, 243 (1994).
7. Corma, A. M. Faraldos, Martinez, A., and Mifsud, A., *J. Catal.* **122**, 230 (1990).
8. Fritz, P. O., and Lunsford, J. H., *J. Catal.* **118**, 85 (1989).
9. Kramer, G. M., McVicker, G. B., and Ziemiak, J. J., *J. Catal.* **92**, 355 (1985).
10. Lombardo, E. A., and Hall, W. K., *J. Catal.* **112**, 565 (1988).
11. Pellet, R. J., Blackwell, C. S., and Rabo, J. A., *J. Catal.* **114**, 71 (1988).
12. Corma, A., Fornes, V., and Rey, F., *Appl. Catal.* **59**, 267 (1990).
13. Chauvin, B., Boulet, M., Massiam, P., Fajula, F., and Courieres, T. D., *J. Catal.* **126**, 532 (1990).
14. Gao, Z., Tang, Y., and Zhu, Y. G., *Appl. Catal.* **56**, 83 (1989).
15. Olson, D. H., Kokatailo, G. T., Lawton, S. L., and Meier, W. M., *J. Phys. Chem.* **85**, 2236 (1981).
16. Zhao, Y. X., Bamwenda, G. R., and Wojciechowski, B. W., *J. Catal.* **142**, 465 (1993).
17. Zhao, Y. X., and Wojciechowski, B. W., *J. Catal.* **144**, 377 (1993).
18. Groten, W. A., and Wojciechowski, B. W., *J. Catal.* **140**, 262 (1993).
19. Higgins, J. B., LaPierre, R. B., Schlenker, J. L., Rohrman, A. C., Wood, J. D., Kerr, G. T., and Rohrbaugh, W. J., *Zeolites* **9**, 350 (1989).
20. Beyerlein, R. A., McVicker, G. B., Yacullo, L. N., and Ziemiak, J. J., *J. Phys. Chem.* **92**, 1967 (1988).
21. Jacobs, P. A., *Catal. Rev.-Sci. Eng.* **24**, 415 (1982).
22. Ko, A. N., and Wojciechowski, B. W., *Prog. React. Kinet.* **12**, 201 (1983).
23. Brunner, E., Ernst, H., Freude, D., Frohlich, T., Hunger, T., and Pfeifer, H., *J. Catal.* **127**, 34 (1991).
24. DeCanio, S. J., John, J. R., Fritz, P. O., and Lunsford, J. H., *J. Catal.* **101**, 132 (1986).
25. Engelhart, J., and Hall, W. K., *J. Catal.* **125**, 472 (1990).
26. Wojciechowski, B. W., *Can. J. Chem. Eng.* **46**, 48 (1968).
27. Wojciechowski, B. W., *Catal. Rev.-Sci. Eng.* **9**(1), 79 (1974).
28. Szepe, S., and Levenspiel, O., *J. Chem. Eng. Sci.* **23**, 881 (1968).
29. Sanz, J., Fornes, A., and Corma, A., *J. Chem. Soc. Faraday Trans. 1* **84**(9), 3113 (1988).
30. Grobet, P. J., Geerts, H., Tielen, M., Martens, J. A., and Jacobs, P. A., *Stud. Surf. Sci. Catal.* **46**, 721 (1989).